Binding of Mazindol and Analogs to the human

Serotonin and Dopamine Transporters.

Kasper Severinsen, Heidi Koldsø, Katrine Almind Vinberg Thorup, Christina Schjøth-Eskesen, Pernille Thornild Møller, Ove Wiborg, Henrik Helligsø Jensen, Steffen Sinning, Birgit Schiøtt

*i*NANO and *in*SPIN Centers, the Department of Chemistry, Aarhus University, Aarhus, Denmark (H.K., B.S); Department of Chemistry, Aarhus University, Aarhus, Denmark (C.S.E., H.H.J.); and Laboratory of Molecular Neurobiology, Translational Neuropsychiatry Unit, Department of Clinical Medicine, Aarhus University Hospital, Risskov, Denmark (K.S., K.A.V.T., P.T.M., O.W., S.S).

1

Running title: Computational and biochemical analysis of Mazindol orientation.

Corresponding authors:

Computational chemistry and biomodeling:

Birgit Schiøtt

Department of Chemistry

Aarhus University

Langelandsgade 140

8000 Aarhus C, Denmark

birgit@chem.au.dk

Fax: +45 8619 6199

Phone: +45 8942 3953

Biochemistry and pharmacology. Correspondance with editors:

Steffen Sinning

Laboratory of Molecular Neurobiology

Translational Neuropsychiatry Unit

Department of Clinical Medicine

Aarhus University Hospital

Skovagervej 2

8240 Risskov, Denmark.

steffen.sinning@cpf.au.dk

Phone: +45 7847 1115.

Text pages: 17

Tables: 4

Figures: 2

References: 60

Abstract: 203 words

Introduction: 761 words

Discussion: 1149 words

Abbreviations: Human serotonin transporter (hSERT), human dopamine transporter (hDAT), human norepinephrine transporter (hNET), human monoamine transporter (hMAT), wildtype (wt), quantum mechanics polarized docking (QPLD), phosphate buffered saline with calcium and magnesium (PBSCM), *Aquifex aolicus* leucine transporter (LeuT), extracellular loop (EL), quantum mechanics (QM), density functional theory (DFT), root mean squared deviation (RMSD), induced fit docking (IFD), standard precision (SP), extra precision (XP), serotonin / 5-hydroxytryptamine (5-HT), paired mutation ligand analog complementation (PaMLAC)

ABSTRACT

Mazindol has been explored as a possible agent in cocaine addiction pharmacotherapy. The tetracyclic compound inhibits both the dopamine transporter and the serotonin transporter and simple chemical modifications alter target selectivity considerably. Mazindol is therefore an attractive scaffold for both understanding the molecular determinants of serotonin/dopamine transporter selectivity and for the development of novel drug abuse treatments. Using molecular modeling and pharmacological profiling of rationally chosen serotonin and dopamine transporter mutants with respect to a series of mazindol analogues has allowed us to determine the orientation of mazindol within the central binding site. We find that mazindol binds in the central substrate binding site, and that the transporter selectivity can be modulated through mutations of a few residues in the binding pocket. Mazindol is most likely to bind as the *R*-enantiomer. Tyrosines 95 and 175 in the human serotonin transporter and the corresponding phenylalanines 75 and 155 in the human dopamine transporter are the primary determinants of mazindol selectivity. Manipulating the interaction of substituents on the 7-position with the human serotonin transporter Tyr175 versus dopamine transporter Phe155 is found to be a strong tool in tuning the selectivity of mazindol analogs and may be utilized in future drug design of cocaine abuse pharmacotherapies.

INTRODUCTION

Abuse of psychostimulants is a huge burden to society resulting in financial, criminal and health problems (Dutta et al., 2003) with cocaine being one of the most powerful reinforcers known to date often leading to dependence and abuse. Cocaine is known to inhibit all three human monoamine transporters (hMATs): the serotonin, norepinephrine and dopamine transporters, hSERT, hNET, and hDAT, respectively. The most important site of action for cocaine is the hDAT, which has lead to the "dopamine hypothesis" (Kuhar et al., 1991) stating that cocaine binds to the transporter and blocks the re-uptake of dopamine leading to an increased concentration of this neurotransmitter in the synaptic cleft. Consequently, an enhancement and a prolonged stimulation of the dopaminergic system occur (Kuhar et al., 1991) causing the strongly reinforcing effect of cocaine. This hypothesis has been verified by knock-in of a cocaine-insensitive DAT (Thomsen et al., 2009; Chen et al., 2006). Several approaches to treat cocaine addiction have been tried, however, none of these have led to compounds used clinically (Kharkar et al., 2008) and an urgent need for the development of drugs against cocaine abuse remains.

The tetracyclic compound mazindol was first synthesized in 1968 (Figure 1). Like cocaine, mazindol binds to all hMATs (Javitch et al., 1984; Angel et al., 1988; Eshleman et al., 1999) and has been shown to be useful as an appetite suppressant and has therefore been used against obesity (Acri, 2008).

Mazindol functions with a favorable rapid rate of onset and binds with a higher affinity to hDAT than cocaine without having significant side-effects (Eshleman et al., 1999; Berger et al., 1989; Chen and Reith, 2002), leading to the speculation that mazindol could be utilized in the treatment of cocaine addiction. Promisingly, mazindol reduces craving and euphoria in cocaine abusing patients in short-term studies (Berger et al., 1989) while results from longer-term studies are not significantly better than the ones observed in placebo treated patients (Stine et al., 1995). Mazindol was shown to cause psychostimulation in monkeys, which might be assigned to a different route of administration, pointing to pharmacokinetics as an important aspect of abuse potential besides DAT inhibition (Dutta et al., 2003; Chait et al., 1987).

Mazindol is selective towards hDAT over hSERT and has been used as a starting molecule in the synthesis of different functionalized analogues by Houlihan *et al* (Houlihan et al., 2002). Novel analogs have been synthesized and tested in this study (Figure 1). Here we explore the binding of mazindol to hDAT and hSERT homology models to determine the molecular determinants of affinity and selectivity. Inhibitory potencies of mazindol and eight analogs (Figure 1) for hSERT

5

and hDAT mutants were explored. Of the original mazindol analogs from Houlihan *et al.* (Houlihan et al., 2002), three have a significant preference for wildtype (wt) hDAT over wt hSERT; compounds; **1**, **2** and **3**, show more than 100-fold preference for hDAT, whereas analog **4**, only shows 36-fold selectivity. The novel analogs reported here where chosen to aid experimental validation of the mazindol binding mode and they generally show lower potency but two analogs show increased selectivity for hSERT. By mutagenesis of a few residues lining the central binding pocket of hSERT, we show that the selectivity of **2**, and to some extent **3**, can be reversed from being predominantly hDAT selective to equipotent against hSERT and hDAT. This tendency can be rationalized from computational studies by means of induced fit docking (IFD) (Sherman et al., 2006) and QM-polarized ligand docking (QPLD) (Cho et al., 2005) calculations of mazindol into homology models of hDAT and hSERT.

The two enantiomers of mazindol and its analogs exist in a dynamic equilibrium between three isomers (the keto and the *R* and *S* –ol forms, respectively) with the *R* or *S*–ol being the only relevant forms at physiological pH (Houlihan et al., 2002). These two enantiomers may have markedly different protein binding affinities, which cannot easily be measured experimentally due their presumed easy interconversion. It was necessary to computationally treat the two enantiomeric –ol forms separately, which predicted that the two enantiomers of mazindol are orientated in similar ways in both proteins. The difference in affinity between the transporters can thereby be assigned to the difference in amino acid composition in the binding pocket at primarily two positions and not to differences in ligand binding. This allows us to present the first biochemically validated binding mode of mazindol and analogues inside the central binding site of hSERT and hDAT pointing to *R*-mazindol as the biologically relevant enantiomer, which may facilitate progress towards the development of anti-abuse drugs.

MATERIALS AND METHODS

The synthesis of **1-4** is described in Houlihan *et al.* (Houlihan et al., 2002)

Organic Synthesis

Mazindol analogs **5**, **6** and **8** were prepared by procedures analogous to those described by Houlihan *et al.* (Houlihan and Parrino, 1982), see Supplementary Information for details.

Crystallography of 5

Please see Supplementary Information for details

Mutagenesis

Mutations in hSERT or hDAT pCDNA inserted into the pCDNA3.1 vector were introduced by mismatched primer pairs in a polymerase reaction using Phusion (Finnzymes). DNA was purified from overnight XL10 Gold E.*coli* cultures grown in LB media supplemented with 200 ng/ml ampicillin using the PureYield midiprep kit (Promega). Mutant DNA was sequenced across the entire transporter open reading frame using BigDye v3.1 chemistry (Applied Biosystems) analyzed on an ABI 3100 sequenzer (Applied Biosystems) to verify that the transporter gene contained the desired mutations and that no unwanted mutations had been introduced.

Cell culture

HEK293MSR cells (Invitrogen) were cultured in Dulbecco's modified Eagle's medium (BioWhitaker) supplemented with 10% fetal calf serum (Invitrogen), 100 units/ml penicillin, 100 µg/ml streptomycin (BioWhitaker), and 6 µg/ml Geneticin (Invitrogen) at 95% humidity and 5% $p(CO_2)$ at 37 °C. Two days prior to the uptake assay, cells were detached by Versene and trypsin/EDTA treatment and mixed with a preformed complex of transporter DNA and Lipofectamine2000 (Invitrogen). This transfection mix was dispensed into TC-treated white 96-well plates (Nunc) at a cell density of 50-70% confluency and 0.167-0.333 µg DNA per cm^2 and incubated for 50-60 hours.

Uptake inhibition assay

Adherent transfected cells were washed with PBSCM (137 mM NaCl, 2.7 mM KCl, 4.3 mM Na_2HPO_4, 1.4 mM KH_2PO_4, 0.1 mM $CaCl_2$ and 1 mM $MgCl_2$ pH 7.4) and preincubated for 25 minutes with a dilution series of the inhibitor. Uptake was initiated by adding a mixture of 50-100 nM [^{3}H]-serotonin or [^{3}H]-dopamine (Perkin Elmer) and the inhibitor at the same concentration as in the preincubation. Radioactive neurotransmitter uptake was allowed to proceed for 10 minutes at 22 °C and terminated by washing with PBSCM. Aspirated cells were lysed with Microscint 20 (Packard) and the accumulated radioactive neurotransmitter quantified on a Packard Topcounter.

Data analysis

Radioactive counts from accumulated neurotransmitter were fitted from to a sigmoidal dose-response curve in Graphpad Prism 3. The resulting IC_{50} values were transformed to K_i values using

7

the Cheng-Prusoff equation. Statistical comparison of Ki values was conducted using Student's t-test.

Molecular Modeling

Homology modeling. One homology model of hDAT and one homology model of hSERT have been utilized in this study. Both models were constructed using the crystal structure of the leucine transporter (LeuT) as a template (Yamashita et al., 2005). The alignment used between LeuT and hSERT and LeuT and hDAT, respectively, was the thoroughly refined one of neurotransmitter sodium symporters published by Weinstein and coworkers (Beuming et al., 2006) and previously been used by us with success (Celik et al., 2008b; Koldsø et al., 2010; Koldsø et al., 2013a; Koldsø et al., 2011; Koldsø et al., 2013b; Severinsen et al., 2012; Sinning et al., 2010).

The hSERT homology model is a further refined model based on our previously validated model of hSERT with serotonin bound (Celik et al., 2008b), including the loop optimization described in Koldsø *et al.* (Koldsø et al., 2010; Koldsø et al., 2013b). The hDAT homology model was constructed by the use of LeuT and the optimized EL2 loop of hSERT as templates and built in MODELLER9v5 (Eswar et al., 2007; Fiser et al., 2002) as previously described (Koldsø et al., 2013b). During the modeling procedure of hDAT, 20 models of the protein were built. The main validation criteria for these models were i) the model quality as measured by the probability density function, molpdf (Eswar et al., 2007), ii) the stereochemical quality illustrated by a Ramachandran plot using PROCHECK (Laskowski et al., 1993), iii) the size of the central cavity binding site of the protein measured the solvent accessible area method with a 1.2 Å probe in Molegro Virtual Docker (www.molegro.com, Molegro Virtual Docker, version MVD2008.2.4; Thomsen and Christensen, 2006), and iv) the χ_1 angle of Asp79 in hDAT which should be $\pm gauche$ as has been previously suggested (Jørgensen et al., 2007; Koldsø et al., 2010; Celik et al., 2008b; Koldsø et al., 2013b).

The sodium ions found in the LeuT crystal structure were imported with the same coordinates into the final hDAT and hSERT models, and the chloride ion was manually introduced in both models at the proposed binding site (Forrest et al., 2007; Zomot et al., 2007) followed by a brief minimization.

Ligand Preparation. Both enantiomers of mazindol were built in Maestro (Maestro, version 8.5, Schrödinger, LLC, New York, NY, 2008.). For macromodel atomtypes for mazindol please see supporting information Fig. S2. The pK_a values of ionizable groups were predicted by Epik 1.6 (Epik, version 1.6, Schrödinger, LLC, New York, NY, 2008.) within the Schrödinger software. The

nitrogen at position 1, N1 (see Figure 1 for atom labeling), had a predicted pK_a value of 9.12 and should be charged at physiological pH. Furthermore, because of the possibility of conjugation and charge delocalization between N1 and N4 in the imidazoline ring, N1 and N4 were chosen to be sp^2-hybridized and thus planar. To investigate the structure of the two enantiomers of mazindol more precisely, a quantum mechanics (QM) optimization was made using the density functional theory (DFT) method B3LYP (Lee et al., 1988; Becke 1993; Stephens et al., 1994) with the 6-31+G(d) basis set (Hehre et al., 1972). The QM optimized structure deviate slightly from planarity around the charged conjugated nitrogen, N1, with a few degrees, which is most likely caused by the intramolecular strain of the tricyclic ring system. The energy minimized structure from the QM optimization was then used as the input for a Monte Carlo Conformational search, using the MCMM methodology in MacroModel 9.6 (MacroModel, version 9.6, Schrödinger, LLC, New York, NY, 2008) with the MMFFs force field in an implicit water model. This specific force field was selected because it has been optimized to keep sp^2-hybridized nitrogens planar (Halgren 1996; Halgren 1999) with atomtypes N4 and N2 to describe the two nitrogen atoms of the imidazoline ring (See Supplemental Figure S2 for details). The conformational search was performed to identify all low energy conformations of mazindol and the global minimum of each enantiomer was used as the input structure for the following IFD simulation.

IFDs with the positive charge localized on N4 have also been performed, see summary in supporting information. These results do, however, not differ from the results from IFD with N1 modeled as positively charged, thus only the results from the latter will be analyzed in detail here.

Protein Preparation. The protein complexes were prepared for docking calculations by the Protein Preparation Wizard in the Schrödinger 2008 suite (Schrödinger Suite 2008 Protein Preparation Wizard). Herein, the protonation states and bond orders of the amino acids were initially predicted and afterwards optimized. The automatically assigned protonation states were used in most cases; however, two residues in both protein complexes were changed manually. These residues were Asp524 and Glu508 in hSERT and Glu396 and Glu491 in hDAT, which, according to PROPKA 2.0 predictions (Li et al., 2005; Bas et al., 2008), both were suggested to be neutral at physiological pH. The protonation state of Glu508 in hSERT and Glu491 in hDAT as neutral is further supported by the finding that similar Glu-Glu pairs are conserved in the NNS family as revealed in the LeuT crystal structure (Forrest et al., 2007). Most histidines in hSERT were retained as the δ-tautomer, except His240, which was modeled as charged. In the model of hDAT, His165, His179, His225, His375, and His444 were all modeled as the ε-tautomer.

Subsequently, each protein was subjected to a constrained minimization within the OPLS-AA force field (Jorgensen and Tirado-Rives, 1988) and converged to an RMSD of 0.3 Å. The refined protein structures were then used as the input structures for following IFD studies.

Induced Fit Docking (IFD) Simulations. Since mazindol is significantly larger than leucine, which was bound inside the binding pocket of the template LeuT, it was thus necessary to include protein flexibility in the docking simulations. The IFD (Schrödinger Suite 2008 Induced Fit Docking protocol; Sherman, et al., 2006) protocol has been utilized throughout this study. In the IFD workflow some side-chain flexibility is introduced for residues with at least one atom within a distance of 5 Å from the ligand. The homology models of hDAT and hSERT do not contain a bound ligand so the binding site was defined by residues previously shown to be important for inhibitor binding, which is Asp98 and Ile172 in hSERT (Henry et al., 2006), and Asp79 and Val152 in hDAT (Lee et al., 2000; Beuming et al., 2008), respectively. The number of poses to save in both the initial and the re-docking stages of the IFD protocol was changed from the default value of 20 to 100. Furthermore, the energy window of the Prime energy in the sorting and filtering step was changed from the default value of 30 kcal/mol to 50 kcal/mol to allow for more diversity among the saved docking poses. The scoring function applied in the initial soft docking was standard precision (SP) (Friesner et al., 2004), whereas the extra precision (XP) scoring function (Friesner et al., 2006) was applied in the re-docking stage of the IFD protocol.

Binding Site Optimization. The binding site of the best docking poses from the IFD calculations, judged from GlideScore and Emodel, were subsequently energy minimized in MacroModel (MacroModel, version 9.6, Schrödinger, LLC, New York, NY, 2008) with the conjugated gradient method until convergence using the OPLS-AA (Jorgensen and Tirado-Rives, 1988) force field with no solvent. The ligand was used to define the center and complete residues in a radius of 8 Å are allowed to move freely during minimization. Surrounding the freely moving area, a shell with a radius of 10 Å was constrained with a force constant of 200 kJ/mol*Å^2 hereby allowing only moderate flexibility of this part of protein structure leaving the rest of the protein frozen during this calculation. The refined protein/ligand complexes were used in the following QPLD docking simulations.

Quantum Polarized Ligand Docking (QPLD). The binding modes identified from the IFD calculations of each enantiomer bound to both of the protein models were then further evaluated by QPLD calculations (Schrödinger Suite 2008 QM-Polarized Ligand Docking protocol). QPLD is a QM/MM based docking method (Cho et al., 2005) combining Glide (Friesner et al., 2004) and

QSite (Murphy et al., 2000). During the QPLD procedure the ligands are initially docked into a rigid protein using Glide. The resulting binding modes of the ligands are then used for calculation of partial charges of the ligand by a single-point calculation in QSite. By this method, the effect of the polarization from the protein experienced by the bound ligand is taken into account in the final docking stage where the partial charges obtained from the QM calculations of the ligand are used. No protein flexibility is possible during the QPLD calculation; however, the ligands are treated as flexible in each of the two docking stages. Three different setups were tested for these calculations exploring the two scoring functions in the initial docking and final re-docking stages. In all setups the center for the grid calculations for the QM/MM step was defined by the position of the ligand in the minimized best structure from the IFD calculations. The number of poses to be returned in each setup is set to 20. The QM level in the QPLD protocol is set to *Accurate*, which implies the DFT method B3LYP (Stephens et al., 1994; Lee et al., 1988; Becke 1993) is applied with the 6-31G(d) basis set.

RESULTS

Molecular modeling. Since mazindol has the positive charge delocalized over two nitrogen atoms, two binding modes can be expected where N1, respectively, N4 interacts with Asp98 in hSERT and Asp79 in hDAT assuming this ionic interaction to be present also for mazindol, similarly to what has previously been found for 5-HT, imipramine, citalopram (Celik et al., 2008b; Sinning et al., 2010; Koldsø et al., 2010; Andersen et al., 2009) in hSERT and for dopamine and cocaine in hDAT (Koldsø et al., 2013b). It has previously been proposed that cocaine binds in a similar fashion to both hDAT and hSERT (Beuming et al., 2008). It can thus be hypothesized that mazindol does that too. Our experimental data (see below) support these findings, so only binding modes identified in both proteins will be analyzed in detail here. One dominating binding mode of *R*-mazindol in hSERT as well as hDAT was identified from the docking calculations where N1 forms an ionic interaction with Asp98 in hSERT, respectively Asp79 in hDAT. This binding mode is termed **R-C1** in the following, see Figure 2, panels B and E. For *R*-mazindol no poses with an ionic interaction below 4.5 Å between N4 and Asp79 in hDAT was found. However, two poses in hSERT were different from **R-C1** and these two, termed **R-C2**, showed an ionic interaction with a distance of less than 4 Å between N4 and Asp98 in hSERT. Since the **R-C2** binding mode is only present in hSERT it will not be analyzed further at this time. The **R-C1** binding mode of mazindol furthermore shows a hydrogen bond between the positive N1 atom of mazindol and the backbone

11

carbonyl group of Phe335 in hSERT and Phe320 in hDAT. Phe335 is one of the two aromatic residues that form an aromatic lid on top of the binding site as observed in the crystal structures of LeuT and other studies (Celik et al., 2008a; Celik et al., 2008b) and it is conserved among almost all neurotransmitter sodium symporters (Yamashita et al., 2005; Beuming et al., 2006). Furthermore, the hydroxyl group at the spiro-centre in **R**-C1 can form a hydrogen bond with the backbone of Ser438 in hSERT and Ser422 in hDAT. The chloro-substituent of mazindol in **R**-C1 resides in a pocket lined by residues Ile165, Ile168, Ala169, Ile172, Phe341, Val343, and Gly442 in hSERT; and Phe76, Ile148, Ser149, Val152, Phe326, Gly327, Val328, Gly425, Gly426, Ser429, in hDAT, all within 5 Å of the chloro-group.

Comparable with observations for *R*-mazindol, one similar binding mode was observed for *S*-mazindol in both hSERT and hDAT with an ionic interaction between N1 and Asp98 and Asp79, respectively. This binding mode is termed **S**-C1. From the IFD calculations in hDAT another binding mode was observed with distances between N4 and Asp79 falling below 4.2 Å, **S**-C2. This cluster will not be analyzed further because of the lack of its presence in both transporters. From the IFD with the positive charged localized on N4 another binding mode, only found in hSERT, was observed, **S**-C3. These poses will not be analyzed further because of the experimental data below and the absence of this binding mode in hDAT. The **S**-C1 binding mode was almost identical between the two different proteins with only a very small variation in the binding pattern; compare Figure 2 panels C and F. In **S**-C1 the hydroxyl group is orientated toward Phe341 in hSERT and Phe326 in hDAT. The positively charged nitrogen in **S**-C1 forms charge reinforced hydrogen bonds with Asp98 in hSERT and Asp79 in hDAT. Furthermore, the chloro substituent in **S**-C1 is located in the pocket surrounded by Ala169, Ala173, and Gly442 in hSERT; and Gly153, Asn157, Ala423, and Met427 in hDAT. The statistics from the different docking setups are listed in Table 1. It is evident that the docking scores are similar for both enantiomers in the dominant clusters, **S**-C1 and **R**-C1, in the two proteins, hSERT and hDAT (see column 8 in Table 1). Additionally, the ionic interaction distance between the N1$^+$ of the ligand and Asp79 and Asp98 in hDAT and hSERT respectively is similar among each enantiomer (see column six in table 1).

In summary, the "core" of mazindol, the fused tricyclic ring system, is predicted to be located in the same orientation inside both proteins for both enantiomers. The major difference between the predicted bindings of the two enantiomers is the orientation of the hydroxyl group and the chloro-phenyl group, thus unequivocal answers may not be expected related to substitutions at the 4′-

position if both enantiomers indeed bind to the protein. From the docking scores, it seems most likely that the two enantiomers of mazindol bind with similar affinities.

Experimental validation of mazindol orientation in hSERT and hDAT.

To validate the predicted binding modes, structure-activity measurements were conducted for a battery of mazindol analogues against hSERT and hDAT mutants. The biochemical experiments were performed with racemic mixtures, however, this is appropriate since the two enantiomeric forms are presumed to be readily interchangeable and to bind with similar affinities.

The Paired Mutation Ligand Analogue complementation (PaMLAC) paradigm was used to validate the binding modes of mazindol in hSERT and hDAT predicted from the docking studies (**S-C1**, **R-C1**, Figure 2). PaMLAC provides a complementary method where a battery of mazindol analogs and complementary protein mutants allow us to extensively investigate the position of specific ligand-protein interaction points. In this study we have used racemic analogs previously described by Houlihan *et al.* (Houlihan et al., 2002) with four novel mazindol analogs (4´ substituent analogs **5-8**). The **5** compound was furthermore crystallized and the structure was solved by crystallography (see Supporting Information). The analogs used to study the binding are substituted either on the "core" of the ligand at position 6, 7 and 9, see Figure 1, or at the para-position (4´-position) of the phenyl group. The mutants used were selected so that the mutated amino acid residue lines the putative binding pocket of the protein. The measured K_i values are listed in Table 2-4.

Orientation of mazindol – tertiary ammonium group:

The possible ionic interaction between the charged N1 position of mazindol and Asp98 in hSERT and Asp78 in hDAT is the dominant docking poses of both enantiomers in both proteins. This type of charge reinforced interaction has previously been seen in other compounds that interact with hSERT (Celik et al., 2008b; Koldsø et al., 2010; Koldsø et al., 2011; Sinning et al., 2010; Koldsø et al., 2013a), hDAT (Beuming et al., 2008) or both (Koldsø et al., 2013b; Severinsen et al., 2012) and the presence of a protonated ammonium group is a hallmark of high affinity inhibitors of SERT and DAT.

hSERT Tyr95/hDAT Phe76 is the primary determinant of mazindol selectivity for hDAT over hSERT

Mazindol is 3.4-fold more selective for hDAT wt than for hSERT wt ($K_{i,hDAT\ wt}$=140 nM vs. $K_{i,hSERT\ wt}$=480 nM, p<0.0001). This selectivity can be fully reversed to a selectivity of 0.11 when introducing the corresponding hDAT residue on hSERT position 95 and the corresponding hSERT

13

residue at the equivalent hDAT position 76 ($K_{i,hDAT\ Phe76Tyr}$=1700 nM vs. $K_{i,hSERT\ Tyr95Phe}$=182 nM, p=0.0002). This shows that Tyr95 in hSERT and the corresponding Phe76 in hDAT is the primary determinant of mazindol selectivity as has already been shown by Randy Blakely and coworkers (Barker et al., 1998). No other single mutant in the binding site of residues diverging between hDAT wt and hSERT wt (see table 2 and 3) shows a similar response but secondary and tertiary mutations in the hSERT Tyr95Phe or hDAT Phe76Tyr background, in particular hDAT Val152Ile, hDAT Met427Leu, hSERT Ile172Val and hSERT Leu443Met, further enhances the response (Table 2-3).

Location of the 6-position by use of **1**:

The location of the 6-position of mazindol in hSERT has been investigated by measuring inhibitory potencies of **1** for wt transporters and single mutant constructs in uptake inhibition experiments. The affinity of **1** in hDAT is 160-fold better than in hSERT with K_i values of 14800 nM in hSERT (Table 2) and 92 nM in hDAT (Table 3). When comparing the inhibitory potency of **1** with the one for mazindol a 31-fold decrease is observed in hSERT, with K_i values of 14800 nM (**1**) and 480 nM (mazindol). The opposite selectivity is observed in hDAT with a very small 1.5-fold increase in potency upon binding of **1** compared to mazindol, with K_i values of 92 nM (**1**) and 140 nM (mazindol). However, some of the lost affinity can be regained in hSERT when introducing the Tyr175Phe mutation. In this situation the affinity is increased 7-fold of the **1** analog compared to wt hSERT ($K_{i,Tyr175Phe}$=2200 nM vs. $K_{i,wt}$=14800 nM, p<0.0001) whereas the effect of introducing the Tyr175Phe mutation is only a limited 1.6-fold increase for mazindol ($K_{i,Tyr175Phe}$=310 nM vs. $K_{i,wt}$=480 nM, p=0.0225). This indicates that the 6-position must be located in a pocket close to Tyr175, which is also observed in the **S-C1** and **R-C1** binding models.

7-position by use of **2**:

The 7-substituted **2** analog inhibits hDAT 113-fold more potently than hSERT, with K_i values of 1940 nM in hSERT and 17.1 nM in hDAT. Additionally, the 7-position of **S-C1** and **R-C1** from IFD and QPLD are located in close proximity to Tyr175 in hSERT and Phe155 in hDAT, see Figure 2. In hSERT wt the introduction of the 7-methoxy as in the **2** analog yields decreased inhibitory potency compared to mazindol corresponding to a 0.25-fold selectivity ($K_{i,mazindol}$ =480 nM vs. $K_{i,2}$ =1940 nM, p<0.0001), whereas the complete opposite selectivity is observed for hDAT wt with a 8.2 selectivity ($K_{i,mazindol}$ =140 nM vs. $K_{i,2}$ =17.1 nM, p<0.0001). These opposite selectivities can be utilized to orient mazindol within the binding site. Ideally, a single mutation in

14

hSERT that could introduce the hDAT-like selectivity in hSERT and conversely the corresponding single mutation in hDAT that could introduce a hSERT-like selectivity for **2** compared to mazindol would be very strong support for a direct interaction between this residue and the 7-position of mazindol. The hSERT Tyr175Phe and corresponding hDAT Phe155Tyr mutations satisfy this PaMLAC criterion fully: For hSERT the mazindol/**2** selectivity shifts from 0.25 for hSERT wt to 4.1 for Tyr175Phe ($K_{i,mazindol}$ =310 nM vs. $K_{i,2}$ =75 nM, p=0.0045). Similarly, for hDAT the mazindol/**2** selectivity shifts from 8.2 for hDAT wt to 0.64 for Tyr175Phe ($K_{i,mazindol}$ =61 nM vs. $K_{i,2}$ =96 nM, p=0.0029). These mirroring reversals of selectivity are highly significant (selectivity of 0.25 vs. 4.1, p<0.0001 and selectivity of 8.1 vs. 0.63, p<0.0001) and experimentally support the computational models, where the 7-position of **S-C1** and **R-C1** mazindol point toward hDAT Phe155 or hSERT Tyr175 and interacts directly with substituents on the 7-position of mazindol.

*Location of the 9-position by use of **3**:*

We have also used analogue **3** to elucidate the effect of the Tyr175Phe mutation in hSERT compared to the reverse mutation Phe155Tyr in hDAT to discern between model **R-C1** and **S-C1**. In **S-C1** the 9-position of mazindol is located less than 3.5 Å from the hydroxyl group on Tyr175 and any substituents on the 9-position would be parallel to this hydroxyl and likely to interact. In **R-C1** the ring system of mazindol is tilted away from Tyr175 and 9-substituents are not likely to interact with the Tyr175 hydroxyl group.

The inhibitory potency of **3** in the wt hSERT compared to mazindol is 2.4-fold decreased, with K_i values of 1140 nM (**3**) and 480 nM (mazindol). Contrary, the inhibitory potency of **3** against wt hDAT is 12-fold higher for the **3** analog compared to mazindol, with K_i values of 11.5 nM (**3**) and 140 nM (mazindol). This analog thus clearly has a distinct selectivity for hDAT. When introducing the Tyr175Phe mutation in hSERT the potency of **3** remains unchanged compared to wt hSERT with K_i values of 1240 nM (Tyr175Phe) and 1140 nM (wt). Similarly, when introducing the corresponding mutation in hDAT, an approximately 2-fold increase in potency of mazindol and **3** is observed compared to wt hDAT, with K_i values of 61 nM and 5.6 nM (Phe155Tyr) compared to 140 nm and 11.5 nM (wt), but no changes in drug selectivity is observed upon introduction of the mutation (hDAT wt selectivity=12 vs. hDAT Phe155Tyr selectivity=10.8). Similarly, hSERT selectivity for **3** compared to mazindol remains constant upon introduction of the hSERT Tyr175Phe mutation (hSERT wt selectivity=480 nM/1140nM=0.42 vs. hSERT Tyr175Phe selectivity=310nM/1240 nM=0.25). This indicates there is no strong interaction between the 9-

position of mazindol and Tyr175 in hSERT and that this residue is not conferring the different selectivity pattern between hSERT and hDAT with respect to 9-substituted analogs which again supports the 9-position as pointing away from the pocket lined by Tyr175 in hSERT and Phe155 in hDAT. These findings do not support the *S*-**C1** model and points to *R*-**C1** model as they are suggested from the computational studies, where the 7-position, and not the 9-position, is oriented toward Tyr175 in hSERT and the corresponding position Phe155 in hDAT, see Figure 2.

Substituents at the Phenyl group:

The *R*-**C1** dockings of *R*-mazindol in hSERT place the electrophilic 4'-chloro substituent in a subpocket lined by Ile168, Ala169, Val343 and partly Phe341while the *S*-**C1** docking of *S*-mazindol in hSERT instead suggests a subpocket lined by Ala173, Gly442, Leu443 and partly Ala169. We decided to identify which subpocket harbours the chloro substituent to determine the most likely stereochemistry of mazindol when bound to hSERT.

To determine the correct binding mode we decided to focus on mutations of Ala169, Asn177 and Val343. Mutations of Gly442 were deemed unsuitable to determine the correct binding mode because mutations of a glycine within an α-helix can have profound effects on the dynamics of the helix but also because Gly442 is located approximately halfway between the two subpockets. Ala169 is also located between the two subpockets and as such cannot be used to unambiguously validate *S*-**C1** over *R*-**C1** or *vice versa* although the models would suggest that the A169 side chain would interact more with the 4'-substituent in *R*-**C1** than *S*-**C1**. We find that the introduction of a hydrophilic residue, in the form of the Ala169Ser mutant, does not significantly affect the potency of mazindol, *5*, *6* or *8* compared to hSERT wt, indicating that the –Cl, -CH$_3$, -OCH$_3$, or -CH$_2$OH is either unable or too large to form a hydrogen bond with the hydroxyl on the serine side chain. However, the introduction of the smaller hydrophilic 4'-hydroxy in *7* allows for a new hydrogen bond that increases the potency of *7* by a factor of 3.4 ($K_{i.hSERT wt}$=12.3 nM vs. $K_{i,A169S}$= 3.6 nM, p=0.0016) and supports the plausibility of both *S*-**C1** and *R*-**C1** and lends support to the notion that *R*-**C1** may be preferred over *S*-**C1.**

Asn177 is located deep in the subpocket harbouring the 4'-chloro group in *S*-**C1** at a distance of more than 6 Å. It is therefore unlikely that any direct interaction between the side chain and the 4'-substituent is possible but mutation of Asn177 might change the overall hydrophilicity or volume of this subpocket. All mutants with smaller residues (Ala, Ser, Thr) at position 177 exhibit significantly increased affinity for the studied analogs (Table 4) but no pattern of hydrophilic side chains pairing favorably with hydrophilic 4'-substituents or hydrophobic side chains pairing

16

favorably with hydrophobic 4'-substituents are found. For the larger but conservative Asn177Gln mutation the same trend of generally improved affinity is observed but much less pronounced than for the Ala, Ser or Thr mutants, indicating that increased volume of the subpocket harbouring the 4'-substituent in **S-C1** is favorable but that no direct interaction between the side chain of residue 177 and the 4'-substituent can be established as predicted by both models.

Val343 is located at the bottom of the subpocket harbouring the 4'-Cl in the **R-C1** pose at a distance of less than 3.5 Å from the chlorine whereas the same distance is in excess of 5.5 Å for **S-C1**. Mutation of the hydrophobic valine to the hydrophilic serine does not in itself affect mazindol potency significantly. Despite the presence of a potential hydrogen bonding partner in Val343Ser the selectivity for the four different 4'-substituent analogs **5-8** compared to mazindol remains unchanged suggesting that the side chain of Val343Ser is unable to interact with the 4'-substituent. This observation disfavors **R-C1** as the correct binding mode.

The models predict that the side chain of Ala173 should have considerable impact on the selectivity for the 4'-substitued analogs for the **S-C1** pose. We observe that the Ala173Leu mutation has a considerable impact on mazindol potency, improving it 37-fold compared to hSERT wt. However, the selectivity for the two hydrophobic analogs (**5** and **6**) or the two hydrophilic analogs (**7** and **8**) of Ala173Leu remains unchanged compared to hSERT wt. Similarly, the selectivity of Ala173Ser for **5-8** is unchanged suggesting that the Ala173 side chain does not interact with 4'-substituents, disfavoring **S-C1**.

DISCUSSION

The IFD and the QPLD calculations of *S*- and *R*-mazindol in hSERT and hDAT resulted in one dominating common binding model for each enantiomer bound to the primary binding site in each of the refined homology models with an ionic interaction between N1 of mazindol and Asp98 (hSERT), respectively Asp79 (hDAT). The predicted binding modes of *R*-mazindol in hSERT and hDAT were similarly oriented. Furthermore, the *S*-mazindol binding mode was also the same in the two protein homology models except from a small spatial displacement. Additionally, the tricyclic scaffold of mazindol molecule was located similarly in both enantiomers and in both protein structures, with all forming an ionic interaction with Asp98 in hSERT and Asp79 in hDAT, respectively.

From extensive SAR studies, it was possible to validate the predicted structure for mazindol in hSERT as well as hDAT using the PaMLAC paradigm. The method does not only rely on isolated

changes in inhibitory potency of analogs but also as a secondary measure links them to the ability of complementary mutations to reverse these changes. Thus, this approach, when successful, adds an extra layer of evidence that provides strong experimental data supporting a direct interaction between a substructure of the ligand and a particular residue side-chain. Conversely, if structural changes to the analog or mutations should induce a different binding mode this is unlikely to result in PaMLAC-derived conclusions at both levels of the evaluation but instead just yield incoherent patterns. As an example, we used the PaMLAC methodology to map three key ligand-protein interactions with high certainty to arrive at an experimentally validated orientation of tricyclic antidepressants in hSERT (Sinning et al., 2010) – the accuracy of this orientation has been verified in a recent crystal structure (Penmatsa et al., 2013) demonstrating the resolution and power of the PaMLAC methodology. By utilizing several analogs we were able to identify the difference between Tyr175 in hSERT and Phe155 in hDAT as being a key reason for the difference in affinity between these two proteins. Mazindol and the analogs all bind to hDAT with greater affinity than to hSERT.

We show that the 6-position is vicinal to hSERT Tyr175Phe just as predicted by poses **R-C1** and **S-C1**. This means that this phenyl group penetrates the aromatic lid composed of hSERT Tyr176 and Phe335 just as has been observed for other inhibitors (Koldsø, et al., 2010; Sinning, et al., 2010) and suggests the same inhibitory mechanism, i.e. inability to close the aromatic lid prevents translocation of the ligand bound to the central substrate site. This proposal is seconded by Gabrielsen *et al* (2012) who have included *R*-Mazindol in the utilization of a flexible docking protocol for different inhibitors of SERT and find one of its aromatic groups to force Tyr176 and Phe335 apart. Furthermore, we observe that a substituent on the 9-position is not sensitive to hSERT Tyr175 mutation as predicted from poses **R-C1** and **S-C1**.

However, the single most striking result is that it was possible to reverse the selectivity of *2* in hSERT by introduction of the Tyr175Phe mutation. This mutation makes this position in hSERT similar to the corresponding position in hDAT, and a large gain in affinity of *2* is observed (26-fold). Similarly, when introducing the Phe155Tyr mutation in hDAT, thereby constructing a hSERT-like architecture of the binding site at this position, potency decreases. Consequently, we suggest that the 7-position of mazindol is oriented toward Tyr175 in hSERT and Phe155 in hDAT as observed in **S-C1** and **R-C1**. Mazindol must, accordingly, bind in very similar ways in both hSERT and hDAT and the difference in amino acid composition must be the key difference in determining the selectivity of these types of compounds inside the binding pocket.

18

With the phenyl part of the tricyclic system extending out through the aromatic lid of the binding site the chlorophenyl moiety is likely to be buried inside the central substrate site. Both **R-C1** and **S-C1** predicts this to be the case, however, with different location of the chloro-group. From Ala169Ser the inhibition data is most consistent with **R-C1**. However, data from Val343Ser could not corroborate this observation whereas inhibition data for Ala173 mutants is mostly consistent with **R-C1**. Therefore, the preponderance of the inhibition data points to **R-C1** as the most likely binding mode and could therefore indicate a preference for the *R*-enantiomer of mazindol. The docking results by Gabrielsen *et al* (2012) suggests an alternative orientation of *R*-Mazindol where the 4´-chlorophenyl protrudes out of the binding site through the aromatic lid in an orientation that is dissimilar to both **S-C1** or **R-C1** in our model. These differing results could be the consequence of the difficulties of different docking protocols to differentiate between two similar aromatic systems and minor differences in the protocols might lead to the aromatic system interchanging in the computations. These discrepancies point to the importance of validation by biochemical experiments. In biochemical experiments we find that a hydroxygroup on the 4´-position can interact favorably, likely through a hydrogen bond, with residue 169 when mutated to a serine. This observation points to the 4´-position being buried in the central binding site, consistent with both **S-C1** and **R-C1**.

Also worth noticing is another disparity in the binding site compositions between hDAT and hSERT, Tyr95 in hSERT corresponds to Phe76 in hDAT. The binding data suggest it is preferable for mazindol analogues to have a phenylalanine at this position since mazindol and all analogs gain affinity when making the Tyr95Phe mutation in hSERT, whereas a decrease in affinity is observed for mazindol and all analogs when introducing the inverted Phe76Tyr mutation in hDAT. This indicates that the property of this aromatic residue is a very important determinant in dictating the selectivity difference between hSERT and hDAT toward mazindol and analogs. In this respect we were able to replicate the results of Barker *et al.* (Barker et al., 1998) who showed that hSERT Tyr95/hDAT Phe76 is an important determinant of SERT/DAT selectivity.

The same trend also holds true when looking at the affinity of cocaine. There is a large increase in affinity of cocaine toward hSERT when introducing the Tyr95Phe mutant, and the opposite effect is observed when incorporating the Phe76Tyr mutant in hDAT. Mazindol has been suggested as an anti-cocaine abuse drug (Berger et al., 1989). Cocaine binds with very similar affinity as mazindol to hSERT, however, mazindol binds 11-fold better than cocaine to hDAT (Eshleman et al., 1999; Houlihan et al., 2002; Chen and Reith, 2002). Since hDAT is the main target for cocaine and

19

mazindol apparently binds to the same site as cocaine (Beuming et al, 2008) it might be able to compete with cocaine and displace it from the binding site. Combined with this favorable profile of mazindol, our findings about mazindol orientation may be used to develop novel ligands based on a mazindol core structure that have a desirable pharmacological profile with respect to potential cocaine addiction pharmacotherapies.

ACKNOWLEDGEMENTS

AUTHORSHIP CONTRIBUTIONS

Participated in research design: K.S., H.K., H.H.J., O.W., B.S. and S.S.

Conducted experiments: K.S., H.K., K.A.V.T., C.S.E., P.T.M. and S.S.

Performed data analysis: K.S., H.K., K.A.V.T., P.T.M., C.S.E., H.H.J., B.S. and S.S.

Wrote or contributed to writing of the manuscript: H.K., H.H.J., S.S. and B.S.

K.S., H.K., K.A.V.T., C.S.E., P.T.M. and S.S. contributed equally.

References

Acri JB (2008) In Vivo Studies of Dopamine Transporter Function, in *Dopamine Transporters: Chemistry, Biology, and Pharmacology* (M. L. Trudell and S. Izenwasser eds) pp 391-437, WILEY, Hoboken, NJ

Andersen J, Taboureau O, Hansen KB, Olsen L, Egebjerg J, Strømgaard K and Kristensen AS (2009) Location of the Antidepressant Binding Site in the Serotonin Transporter: Importance of Ser-438 in the recognition of citalopram and tricyclic antidepressants. *J Biol Chem* **284:**10276-10284.

Angel I, Taranger M, Claustre Y, Scatton B and Langer SZ (1988) Anorectic activities of serotonin uptake inhibitors: Correlation with their potencies at inhibiting serotonin uptake and ^{3}H-mazindol binding. *Life Sci* **43:**651-658.

Barker EL, Perlman MA, Adkins EM, Houlihan WJ, Pristupa ZB, Niznik HB and Blakely RD (1998) High Affinity Recognition of Serotonin Transporter Antagonists Defined by Species-scanning Mutagenesis. *J Biol Chem* **273:**19459-19468.

Bas DC, Rogers DM and Jensen JH (2008) Very fast prediction and rationalization of pK_a values for protein-ligand complexes. *Proteins: Structure, Function, and Bioinformatics* **73:**765-783.

Becke AD (1993) Density-functional thermochemistry. III. The role of exact exchange. *J Chem Phys* **98:**5648-5652.

Berger P, Gawn F and Kosten TR (1989) Treatment of Cocaine Abuse with Mazindol. *Lancet* **1:**283.

Beuming T, Kniazeff J, Bergmann ML, Shi L, Gracia L, Raniszewska K, Newman AH, Javitch JA, Weinstein H, Gether U and Loland CJ (2008) The binding sites for cocaine and dopamine in the dopamine transporter overlap. *Nat Neurosci* **11:**780-789.

21

Beuming T, Shi L, Javitch JA and Weinstein H (2006) A Comprehensive Structure-Based Alignment of Prokaryotic and Eukaryotic Neurotransmitter/Na$^+$ Symporters (NSS) Aids in the Use of the LeuT Structure to Probe NSS Structure and Function. *Mol Pharmacol* **70:**1630-1642.

Celik L, Schiøtt B and Tajkhorshid E (2008a) Substrate binding and formation of an occluded state in the leucine transporter. *Biophys J* **94:**1600-1612.

Celik L, Sinning S, Severinsen K, Hansen C, Møller M, Bols M, Wiborg O and Schiøtt B (2008b) Binding of Serotonin to the Human Serotonin Transporter. Molecular Modeling and Experimental Validation. *J Am Chem Soc* **130:**3853-3865.

Chait LD, Uhlenhuth EH and Johanson CE (1987) Reinforcing and subjective Effects of Several Anorectics in Normal Human Volunteers. *J Pharmacol Exp Ther* **242:**777-783.

Chen N and Reith MEA (2002) Structure-Function Relationship for Biogenic Amine Neurotransmitter Transporters, in *Neurotransmitter Transporters: Structure, Function, and Regulation* (M. E. A. Reith ed) pp 53-109, Humana Press, Totowa, NJ.

Chen R, Tilley RC, Wei H, Zhou F, Zhou F-, Ching S, Quan N, Stephens RL, Hill ER, Nottoli T and Han, D. D. and Gu, H. H. (2006) Abolished cocaine reward in mice with a cocaine-insensitive dopamine transporter. *Proc Natl Acad Sci U S A* **103:**9333-9338.

Cho AE, Guallar V, Berne BJ and Friesner R (2005) Importance of accurate charges in molecular docking: Quantum mechanical/molecular mechanical (QM/MM) approach. *J Comput Chem* **26:**915-931.

Dutta AK, Zhang S, Kolhatkar R and Reith MEA (2003) Dopamine transporter as target for drug development of cocaine dependence medications. *Eur J Pharmacol* **479:**93-106.

Epik, version 1.6, Schrödinger, LLC, New York, NY, 2008.

Eshleman AJ, Carmolli M, Cumbay M, Martens CR, Neve KA and Janowsky A (1999) Characteristics of drug interactions with recombinant biogenic amine transporters expressed in the same cell type. *J Pharmacol Exp Ther* **289:**877-885.

Eswar N, Webb B, Marti-Renom MA, Madhusudhan MS, Eramian D, Shen M, Pieper U and Sali A (2007) Comparative Protein Structure Modeling Using MODELLER. *Curr Protocol Prot Sci* **2:**1-2. 9.

Fiser A, Feig M, Brooks CL 3rd and Sali A (2002) Evolution and Physics in Comparative Protein Structure Modeling. *Acc Chem Res* **35:**413-421.

Forrest LR, Tavoulari S, Zhang YW, Rudnick G and Honig B (2007) Identification of a chloride ion binding site in Na$^+$/Cl$^-$-dependent transporters. *Proc Natl Acad Sci USA* **104:**12761-12766.

Friesner RA, Banks JL, Murphy RB, Halgren TA, Klicic JJ, Mainz DT, Repasky MP, Knoll EH, Shelley M, Perry JK, Shaw DE, Francis P and Shenkin PS (2004) Glide: A New Approach for Rapid, Accurate Docking and Scoring. 1. Method and Assessment of Docking Accuracy. *J Med Chem* **47:**1739-1749.

Friesner RA, Murphy RB, Repasky MP, Frye LL, Greenwood JR, Halgren TA, Sanschagrin PC and Mainz DT (2006) Extra Precision Glide: Docking and Scoring Incorporating a Model of Hydrophobic Enclosure for Protein-Ligand Complexes. *J Med Chem* **49:**6177-6196.

Gabrielsen M, Kurczab R, Ravna AW, Kufareva I, Abagyan R, Chilmonczyk Z, Bojarski AJ and Sylte I (2012) Molecular mechanism of serotonin transporter inhibition elucidated by a new flexible docking protocol. *Eur J Med Chem* **47**(1): 24-37.

Halgren TA (1999) MMFF VII. Characterization of MMFF94, MMFF94s, and Other Widely Available Force Fields for Conformational Energies and for Intermolecular-Interaction Energies and Geometries. *J Comput Chem* **20:**730-748.

23

Halgren TA (1996) Merck Molecular Force Field: I. Basis, form, scope, parameterization and performance of MMFF94. *J Comput Chem* **17:**490-519.

Hehre WJ, Ditchfield R and Pople JA (1972) Self-Consistent Molecular Orbital Methods. XII. Future Extensions of Gaussian-Type Basis Sets for Use in Molecular Obital Studies of Organic Molecules. *J Chem Phys* **56:**2257-2261.

Henry LK, Field JR, Adkins EM, Parnas ML, Vaughan RA, Zou MF, Newman AH and Blakely RD (2006) Tyr95 and Ile172 in transmembrane segments 1 and 3 of human serotonin transporters interact to establish high-affinity recognition of antidepressants. *J Biol Chem* **281:**2012-2023.

Houlihan WJ and Parrino VA (1982) Directed Lithiation of 2-Phenyl- and 2-(*o*-Methylphenyl)imidazoline. *J Org Chem* **47:**5177-5180.

Houlihan WJ, Kelly L, Pankuch J, Koletar J, Brand L, Janowsky A and Kopajtic TA (2002) Mazindol Analogues as Potential Inhibitors of the Cocaine Binding Site at the Dopamine Transporter. *J Med Chem* **45:**4097-4109.

Javitch JA, Blaustein RO and Snyder SH (1984) [³H]mazindol binding associated with neuronal dopamine and norepinephrine uptake sites. *Mol Pharmacol* **26:**35-44.

Jørgensen AM, Tagmose L, Jørgensen AMM, Topiol S, Sabio M, Gundertofte K, Bøgesø KP and Peters GH (2007) Homology Modeling of the Serotonin Transporter: Insights into the Primary Escitalopram-binding Site. *ChemMedChem* **2:**815-826.

Jorgensen WL and Tirado-Rives J (1988) The OPLS potential functions for proteins - energy minimizations for crystals of cyclic-peptides and crambin. *J Am Chem Soc* **110:**1666-1671.

Kharkar PS, Dutta AK and Reith MEA (2008) Structure-Activity Relationship Study of Piperidine Derivates for Dopamine Transporters, in *Dopamine Transporters: Chemistry, Biology, and Pharmacology* (M. L. Trudell and S. Izenwasser eds) pp 233-264, WILEY, Hoboken, NJ

Koldsø H, Autzen HE, Grouleff J and Schiøtt B (2013a) Ligand induced conformational changes of the human serotonin transporter revealed by molecular dynamics simulations. *PLOS ONE* **8**(6): e63635. doi:10.1371/journal.pone.0063635

Koldsø H, Christiansen AB, Sinning S and Schiøtt B (2013b) Comparative modelling of the human monoamine transporters: similarities in substrate binding. *ACS Chem Neurosci* **4:**295-309.

Koldsø H, Noer P, Autzen HE, Grouleff J, Sinning S and Schiøtt B (2011) Unbiased Simulations Reveal the Inward-facing Conformation of the human Serotonin Transporter and Na$^+$ Ion Release. *PLoS Comp Biol* **7(10):**e1002246.

Koldsø H, Severinsen K, Tran TT, Celik L, Jensen HH, Wiborg O, Schiøtt B and Sinning S (2010) The Two Enantiomers of Citalopram Bind to the human Serotonin Transporter in Reversed Orientations. *J Am Chem Soc* **132:**1311-1322.

Kuhar MJ, Ritz MC and Boja JW (1991) The dopamine hypothesis of the reinforcing properties of cocaine. *Trends Neurosci* **14:**299-302.

Laskowski RA, MacArthur MW, Moss DS and Thornton JM (1993) PROCHECK: a program to check the stereochemical quality of protein structures. *J Appl Cryst* **26:**283-291.

Lee C, Yang W and Parr RG (1988) Development of the Colle-Salvetti correlation-energy formula into a functional of the electron density. *Phys Rev B* **37:**785-789.

Lee S, Chang M, Lee K, Park BS, Lee Y, Chin HR and Lee Y (2000) Importance of Valine at Position 152 for the Substrate Transport and 2beta -Carbomethoxy-3beta -(4-fluorophenyl)tropane Binding of Dopamine Transporter. *Mol Pharmacol* **57:**883-889.

Li H, Robertson AD and Jensen JH (2005) Very fast empirical prediction and rationalization of protein pK_a Values. *Proteins: Struct Funct Bioinf* **61:**704-721.

MacroModel, version 9.6, Schrödinger, LLC, New York, NY, 2008.

Maestro, version 8.5, Schrödinger, LLC, New York, NY, 2008.

Murphy RB, Philipp DM and Friesner RA (2000) A mixed quantum mechanics/molecular mechanics (QM/MM) method for large-scale modeling of chemistry in protein environments. *J Comput Chem* **21:**1442-1457.

Penmatsa A, Wang KH and Gouaux E (2013) X-ray structure of dopamine transporter elucidates antidepressant mechanism. *Nature*.

Schrödinger Suite 2008 Induced Fit Docking protocol, Glide version 5.0, Schrödinger, LLC, New York, NY, 2005 and Prime version 1.7, Schrödinger, LLC, New York, NY, 2005

Schrödinger Suite 2008 QM-Polarized Ligand Docking protocol, Glide version 5.0, Schrödinger, LLC, New York, NY, 2008, Jaguar version 7.5, Schrödinger, LLC, New York, NY, 2008 and QSite version 5.0, Schrödinger, LLC, New York, NY, 2008.

Schrödinger Suite 2009 Protein Preparation Wizard, Epik version 2.0, Schrödinger, LLC, New York, NY, 2009, Impact version 5.5, Schrödinger, LLC, New York, NY, 2009 and Prime version 2.1, Schrödinger, LLC, New York, NY, 2009.

Severinsen K, Kraft JF, Koldsø H, Vinberg KA, Rothman RB, Partilla JS, Wiborg O, Blough B, Schiøtt B and Sinning S (2012) Binding of the Amphetamine-like 1-Phenyl-piperazine to Monoamine Transporters. *ACS Chem Neurosci* **3:**693-705.

Sherman W, Day T, Jacobson MP, Friesner RA and Farid R (2006) Novel Procedure for Modeling Ligand/Receptor Induced Fit Effects. *J Med Chem* **49:**534-553.

Sinning S, Musgaard M, Jensen M, Severinsen K, Celik L, Koldsø H, Meyer T, Bols M, Jensen HH, Schiøtt B and Wiborg O (2010) Binding and orientation of tricyclic antidepressants within the central substrate site of the human serotonin transporter. *J Biol Chem* **285:**8363-8374.

Stephens PJ, Devlin FJ, Chabalowski CF and Frisch MJ (1994) Ab Initio Calculation of Vibrational Absorption and Circular Dichroism Spectra Using Density Functional Force Fields. *J Phys Chem* **98:**11623-11627.

Stine SM, Krystal JH, Kosten TR and Charney DS (1995) Mazindol treatment for cocaine dependence. *Drug Alcohol Depend* **39:**245-252.

Thomsen M, Han DD, Gu HH and Caine SB (2009) Lack of Cocaine Self-Administration in Mice Expressing a Cocaine-Insensitive Dopamine Transporter. *J Pharmacol Exp Ther* **331:**204-211.

Thomsen R and Christensen MH (2006) MolDock: A New Technique for High-Accuracy Molecular Docking. *J Med Chem* **49:**3315-3321.

www.molegro.com, Molegro Virtual Docker, version MVD2008.2.4

Yamashita A, Singh SK, Kawate T, Jin Y and Gouaux E (2005) Crystal structure of a bacterial homologue of Na^+/Cl^--dependent neurotransmitter transporters. *Nature* **437:**215-223.

Zomot E, Bendahan A, Quick M, Zhao Y, Javitch J and Kanner B (2007) Mechanism of chloride interaction with neurotransmitter:sodium symporters. *Nature* **449:**726-730.

FOOTNOTES

Address correspondence to:

Professor Birgit Schiøtt. E-mail: birgit@chem.au.dk, fax: +45 8619 6199, phone: +45 8942 3953.

Assistant professor Steffen Sinning. E-mail: steffen.sinning@cpf.au.dk, phone: +45 7847 1115.

MOL #88922

LEGENDS FOR FIGURES

Figure 1: (A) Chemical structures and atom numbering of mazindol and analogs used in this study and (B) chemical structures of protonated serotonin, dopamine and cocaine.

Figure 2: The binding mode of mazindol in hSERT and hDAT. (A) The homology model of hSERT. The TM parts forming the binding site are highlighted with TM1 in pink, TM3 in purple, TM6 in green, and TM8 in yellow. (B) *R*-mazindol bound in hSERT is shown with selected residues lining the binding pocket. **R-C1** is shown in orange and the protein in light gray. (C) *S*-mazindol bound in hSERT is shown with selected residues around the binding pocket. **S-C1** is shown in green and the protein in light gray. (D) The homology model of hDAT. The TM parts forming the binding site are highlighted with TM1 in pink, TM3 in purple, TM6 in green, and TM8 in yellow. (E) *R*-mazindol in hDAT is shown with selected residues of the binding pocket. **R-C1** is shown in orange and the protein in dark grey. (F) *S*-mazindol in hDAT is shown with selected residues of the binding pocket. **S-C1** is shown in green and the protein in dark grey.

Table 1. Statistics for the clusters identified from the different setups applied. The mean value is listed for the distance, GlideScore and Emodel. Furthermore standard deviations are shown in brackets. Data for all poses are included in the Supplementary Information.

Cluster	Protein	Method	Scoring function Initial docking/ re-docking	Number of poses/total poses	Distance Asp98(Oδ)-N1$^+$ (Å)	Distance Asp98(Oδ)- N4 (Å)	GlideScore (kcal/mol)	Emodel (kcal/mol)
R-C1	hSERT							
		IFD	SP/XP	11/17	3.13 [0.19]	4.20 [0.25]	-10.4 [1.2]	-53.7 [17.9]
		QPLD	SP/SP	20/20	4.05 [0.71]	4.67 [0.12]	-9.6 [1.1]	-77.77 [15.0]
		QPLD	SP/XP	10/10	3.43 [0.04]	4.59 [0.03]	-10.5 [0.1]	-75.3 [1.7]
		QPLD	XP/XP	1/1	3.45 [-]	4.60 [-]	-10.5 [-]	-76.3 [-]
S-C1	hSERT							
		IFD	SP/XP	4/12	2.98 [0.40]	4.67 [0.31]	-8.6 [1.7]	-33.1 [26.1]
		QPLD	SP/SP	11/20	2.70 [0.07]	4.60 [0.08]	-9.3 [0.5]	-90.1 [6.9]
		QPLD	SP/XP	6/6	2.73 [0.10]	4.63 [0.08]	-9.9 [0.1]	-68.7 [1.7]
		QPLD	XP/XP	2/2	2.72 [0.05]	4.65 [0.03]	-10.0 [0.0]	-69.4 [1.3]
R-C1	hDAT							
		IFD	SP/XP	2/12	3.34 [0.09]	3.11 [0.36]	-9.8 [0.4]	-49.5 [9.0]
		QPLD	SP/SP	17/20	3.62 [0.35]	3.52 [0.06]	-9.2 [1.9]	-74.5 [20.0]
		QPLD	SP/XP	9/9	3.49 [0.02]	3.51 [0.03]	-10.7 [0.1]	-71.3 [5.7]
		QPLD	XP/XP	2/2	3.52 [0.00]	3.52 [0.01]	-10.8 [0.1]	-75.5 [0.7]
S-C1	hDAT							
		IFD	SP/XP	4/24	2.94 [0.20]	4.77 [0.28]	-9.3 [0.7]	-35.9 [21.0]
		QPLD	SP/SP	10/20	2.80 [0.08]	4.76 [0.06]	-10.3 [0.2]	-84.0 [3.3]
		QPLD	SP/XP	10/10	2.78 [0.06]	4.74 [0.04]	-9.9 [0.4]	-62.1 [3.9]
		QPLD	XP/XP	2/2	2.82 [0.10]	4.77 [0.06]	-9.9 [0.6]	-65.2 [1.2]

30

Table 2. K$_i$ values (nM) from ^{3}H-serotonin uptake inhibition experiments in hSERT wt and hSERT mutations of residues in the central binding site diverging between hSERT and hDAT. Confidence levels are found in the Supporting Information Table S2.

	K$_i$ values 5-HT uptake(nM)				
	Mazindol	*1*	*2*	*3*	*4*
WT	480	14800	1940	1140	2500
Y95F	182	2000	230	98	159
A169S	230	15500	760	740	1500
I172V	270	10000	830	430	610
A173G	850	6900	1560	490	2080
Y175F	310	2200	75	1240	310
T439A	590	8900	840	830	4100
L443M	380	7200	1340	1770	590
T497A	189	4400	165	119	1240
Y95F_I172V	78	4300	220	36	310
Y95F_L443M	210	3200	170	72	250
I172V_L443M	360	17900	290	270	830
Y95F_I172V_L443M	77	4000	157	27	360

Table 3. K_i values (nM) from ^{3}H-dopamine uptake inhibition experiments in hDAT wt and hDAT mutations of residues in the central binding site diverging between hSERT and hDAT. Confidence levels are found in the Supporting Information Table S3.

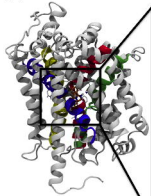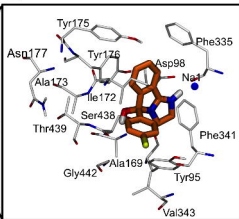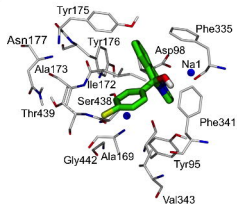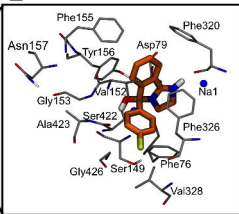|	K_i values DA uptake(nM)				
	Mazindol	*1*	*2*	*3*	*4*
WT	140	92	17.1	11.5	68
F76Y	1700	260	52	71	177
S149A	196	210	21	13.4	71
V152I	80	37	5.4	6.5	33
G153A	340	76	12.7	7.7	94
F155Y	61	59	96	5.6	14.7
A423T	69	16.8	5.1	5.4	14.0
M427L	290	101	21	13.4	88
A480T	82	13.4	7.7	5.7	8.1
F76Y_V152I	5700	1400	230	230	1200
F76Y_M427L	4100	550	76	127	450
V152I_M427L	159	68	10.6	7.5	44
F76Y_V152I_M427L	17400	1660	163	204	2300

32

Table 4. K_i values (nM) from serotonin and dopamine uptake inhibition experiments in hDAT wt, hSERT wt and mutants. Residues Val343, Thr439, Leu443 and possibly Asn177 are suggested by *S-C1* to interact with the 4'-substituent on Mazindol, whereas A173, and possibly Ile165 are suggested by **R-C1** to interact with the 4'-substituent on Mazindol. Ala169 is located between the 4'-substituent on Mazindol in **R-C1** and **S-C1**. Confidence levels are found in the Supporting Information Table S4. ND = Not determined.

	K_i values, 5-HT or DA uptake(nM)				
	Mazindol	*5*	*6*	*7*	*8*
hSERT wt	0.48	5.4	1.92	12.3	21
N177A	0.073	0.150	0.39	2.7	ND
N177S	0.035	0.27	0.26	6.7	3.0
N177T	0.028	0.20	0.22	5.0	4.6
N177Q	ND	ND	1.43	5.9	13.6
T439A	1.24	2.5	0.94	3.4	5.1
T439S	0.92	1.34	0.31	2.44	4.3
T439V	0.24	2.1	0.87	3.5	5.4
L443S	1.05	4.5	1.11	5.3	8.3
A169S	0.48	4.8	3.4	3.6	27
I165A	0.144	1.72	0.72	0.58	6.6
I165S	0.145	2.0	1.08	3.1	9.0
I165T	0.182	1.72	0.77	2.2	4.4
I165N	0.183	2.8	0.70	2.2	17.2
A173S	0.32	1.54	1.41	12.1	15.9
A173L	0.0132	0.062	0.035	0.47	0.55
A173M	ND	ND	ND	ND	0.94
V343S	0.49	8.4	3.1	11.5	28

33

hDAT	0.140	1.27	3.8	35.5	14.5

34
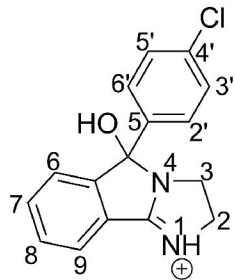
A: Mazindol, *1*, *2*, *3*, *4*, *5*, *6*, *7*, *8*
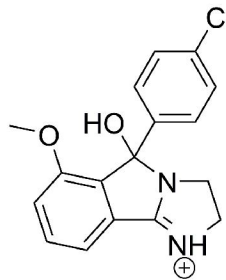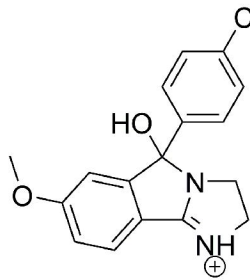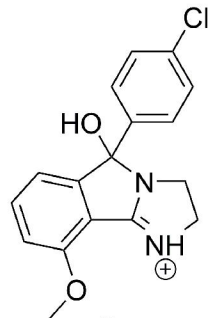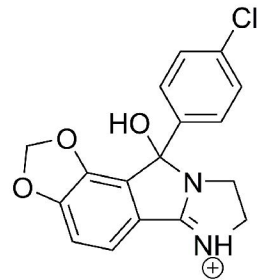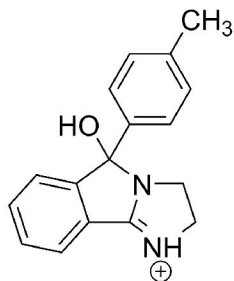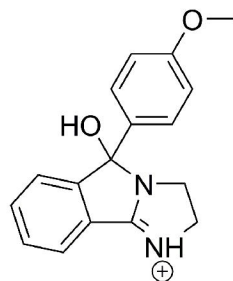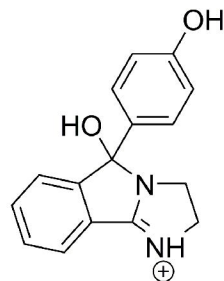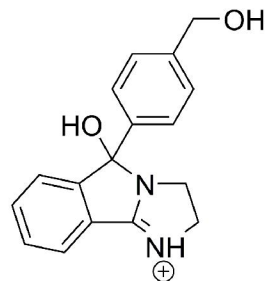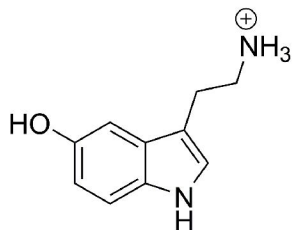
B: Serotonin, Dopamine, Cocaine

Figure 1

Figure 2